# SUBCRITICAL BORON EXPERIMENTS IN THE IPEN/MB-01 REACTOR

A. DOS SANTOS, G.S. SOUZA, D.F. SANTOS, D.A. ANDRADE

*Instituto de Pesquisas Energéticas e Nucleares*
*Av. Prof. Lineu Prestes, 2242 CEP 05508000 São Paulo, SP, Brasil*

## ABSTRACT

Macroscopic (APSD and CPSD) and microscopic (Rossi-α) neutron noise experiments were performed in the IPEN/MB-01 reactor in order to measure subcritical reactivities. Subcritical states of up to around -6600 pcm were reached with insertion of boric acid ($H_3BO_3$) into the moderator tank. The subcritical kinetic model of Gandini and Salvatores was employed to infer the relative power between two consecutive subcritical cases, the subcritical reactivity ($\rho_{gen}$), and the subcriticality index ($\zeta$). This experimental methodology to measure these parameters was successfully employed in a previous experiment performed in the IPEN/MB-01 reactor. The measured subcritical reactivities are in good agreement for the APSD and Rossi-α cases. However, some drawbacks were found for the CPSD cases due to difficulties in the establishment of the cutoff frequency. The MCNP6.1 calculated subcritical reactivities were in a good agreement to APSD´s and Rossi-α measurement values. The ENDF/B-VII.0 nuclear data library was employed in all cases.

## 1. Introduction

Subcritical experiments and the corresponding keff inference are important in a great variety of applications. For example, the monitoring and the prediction of the subcritical multiplication conditions are essential to assure that the operation of the control rod withdrawn, or the boron dilution processes are carried out with safety in order to get criticality of the reactor core. Currently, there are several methods able to estimate the subcritical reactivity [1,2,3]. Subcritical measurement techniques in deeply subcritical systems (negative reactivities less than 10,000 pcm) constitute one of the last frontiers in Reactor Physics. Many techniques have been proposed, but none of them has been successfully considered acceptable to fulfil the requirements of benchmarks. Subcritical reactivity is not a quantity that is measured directly. Instead it is inferred from the detector signals and a kinetic model. Subcritical reactivity measurements can be split into three major categories: a) Static or Quasi-Static Methods such as SMM – Source Multiplication Method and MSM [4] – Modified Source multiplication Method [1], b) Dynamic Methods [5], and c) Neutron Noise Methods [6].

The static or quasi-static methods rely mostly in the detector signals placed strategically around or inside of the reactor core. The reactor system is considered at steady state and the detector responses mainly counts, are collected for further analyses. The main assumption is that detector count rates are linked to sub-critical levels, and, consequently, count rate variations are linked to reactivity variation between two configurations. This is the main hypotheses for the development of the Source Multiplication Method. This is the simplest method to measure the subcritical from the three categories mentioned above. Extensions of this technique considers the Modified Source Multiplication (MSM) method and the Amplified Source Multiplication (ASM). These techniques require calculated correction factor which might impose severe bias in the measured results.

The dynamic method is based on the analysis of the time response of detectors placed in the reactor after a source neutron pulse. The evolution of the detector count rates strongly reflects that of the neutron population over time. The technique assumes that the neutron point kinetics can represent the neutron population evolution over time after a pulse (considered as a Dirac peak). The Area method (also referred as the Sjöstrand method) [5] allows one to determine in a straightforward way the reactivity (in units of dollar) of a subcritical nuclear reactor with no input from theoretical calculations, as long as the assumptions of the neutron point kinetics hold in the reactor. Although the area method is an old and well known technique, giving good results for subcritical reactivities measurements, spatial effects concerning detector and source positions should be taken into account in some cases, mainly for detectors in the reflector regions.

The neutron noise methods rely on the measurements of the neutron density fluctuations in the nuclear reactor. The experimental techniques usually employ macroscopic noise techniques through the determination of the spectral densities APSD (Auto Power Spectral Density) and CPSD (Cross Power Spectral Density) or the microscopic through the determination of the Rossi-α curve or the Feynman-Y curve method.

A common characteristic of these subcritical measurement categories is that they rely on the validity of the point kinetic model and a single decay mode (α-mode) which is not applicable in all situations. Also, calculated correction factors and the determination of the detector efficiency play an important role in these techniques.

The subcritical reactivity is closely related to the kinetic model applicable to the system. Several models [7, 8] were proposed to characterize the kinetics of subcritical reactors especially in regard to the reactivity of the system. Theoretical models suggest the unfolding of the system reactivity into two components: first, the reactivity of a system as normally obtained through the generalized perturbation theory [9] and second, the reactivity due to the source present in the system. This last component is extremely complex to obtain experimentally since the detector's efficiency is altered when the subcriticality level of the system changes. An experimental procedure based on these recent subcritical kinetic models proved successful up to -5,000 pcm was developed by dos Santos et. al. [10]. This proposed method does not require any sort of correction factors neither the knowledge of the detector efficiencies. The only hypotheses made are that the prompt neutron generation ($\Lambda$) and the effective delayed neutron fraction ($\beta_{eff}$) are assumed to be independent of the subcritical reactivity level.

The purpose of this work is to apply a recent technique developed in the IPEN/MB-01 facility to measure subcritical reactivities [10] based on the subcritical model of Gandini and Salvatores [7]. The developed method was based on the measurements of the APSD in the reflector region of the reactor. Extensions of this experimental technique are made in this work by introducing Rossi-α and CPSD measurements. The experiments considered in this work consider the dilution of soluble boric acid in the moderator tank in order to make the reactor subcritical.

## 2. The IPEN/MB-01 core configuration

The core configuration considered a short version of the IPEN/MB-01 core in a 26x24 rectangular array of fuel rods as shown in Figure 1. For this experiment the outer row of fuel rods was removed in each face from the standard IPEN/MB-01 configuration (28x26), i.e., 104 fuel rods. Thus, almost all of reactivity excess was removed from the core (measured $k_{eff}$ is equal to 1.00010, with control and safety banks completely withdrawn). Two $^{3}$He centronic detectors were employed to get the neutron counts for the IPEN/MB-01 correlator. The counts were then summed in order to get better statistics in the measurements.

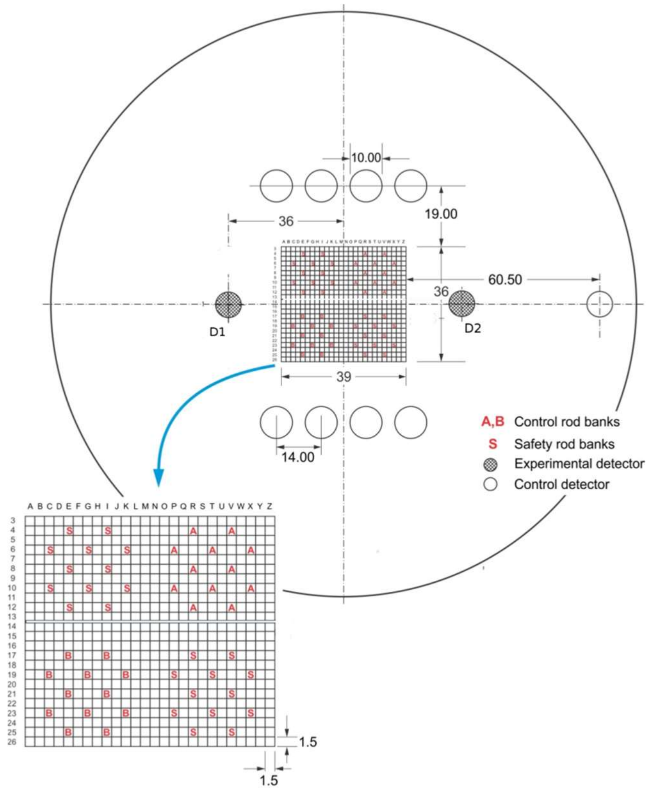


Fig 1. Upper view of the core of the IPEN/MB-01 reactor

A complete description of the IPEN/MB-01 core can be found elsewhere [11].

## 3. The subcritical reactivity inferences

The Gandini and Salvatores [7] subcritical kinetic equations are given by:

$$\Lambda \frac{dP_N(t)}{dt} = (\rho_{gen} - \beta_{eff})P_N(t) + \sum_{j=1}^{NF} \lambda_j \xi_j(t) + \zeta(1 - P_N(t)) + \rho_{source} \tag{1}$$

and

$$\frac{d\xi_j(t)}{dt} = \beta_{eff} P_N(t) - \lambda_j \xi_j(t) \tag{2}$$

where:
$\Lambda$ : the prompt neutron generation time,
$P_N(t)$ : the relative power of the reactor,
$\rho_{gen}$ : the generalized reactivity between two consecutive subcritical states; i.e. the reactivity arising from the generalized perturbation theory (GPT),
$\beta_{eff}$: the effective fraction of delayed neutrons,
$\beta_{eff,j}$: the effective fraction of $j^{th}$ family of delayed neutrons,
$\lambda_j$ : the precursor decay constant for the $j^{th}$ family of delayed neutrons,
$\xi_j$ : the concentration of the precursor of the $j^{th}$ family of delayed neutrons,
$\zeta$ : the subcriticality index, and
$\rho_{source}$ : the reactivity due to variation of the source.

The method developed in the IPEN/MB-01 reactor considered for the inference of the subcritical reactivity considers two consecutive subcritical states *a* and *b*. Here the state *b* is more subcritical than state *a*. $\zeta$ is the subcriticality index for state *a*. According to Ref. 10, the generalized reactivity ($\rho_{gen}$) for these consecutive subcritical states and the subcriticality index ($\zeta$) for state *a* can be determined as:

$$\rho_{gen} = (B\Lambda + \beta_{eff})(1 - P_N) \tag{3}$$

$$\zeta = -(B\Lambda + \beta_{eff})\, P_N \tag{4}$$

The relative power between these two subcritical states is given by:

$$P_N = \frac{P_b}{P_a} = \frac{R_b^2 B_a^2 (\Phi_a^p - C_a)}{R_a^2 B_b^2 (\Phi_b^p - C_b)} \tag{5}$$

where

$R_j$ is the pulse detector counts in step *j*,

*B* is the prompt neutron decay constant,

$\Phi^p =$ mean value of the APSD on the first plateau level in Counts$^2$/Hz for pulse mode detector,

*C* = mean value of the uncorrelated noise.

The uncertainties on $\rho_{gen}$ and $\zeta$ were calculated through the standard error propagation of Eqs. (3) and (4), respectively as:

$$\sigma^2_{\rho_{gen}} = \left[(B_b l_{eff} + \beta_{eff})P_N\right]^2 \left[2^2\left(\frac{\sigma^2_{R_b}}{R_b^2} + \frac{\sigma^2_{R_a}}{R_a^2} + \frac{\sigma^2_{B_a}}{B_a^2}\right) + \frac{\sigma^2_{C_b} + \sigma^2_{\Phi_b}}{(\Phi_b - C_b)^2} + \frac{\sigma^2_{C_a} + \sigma^2_{\Phi_a}}{(\Phi_a - C_a)^2}\right] \\ + \sigma^2_{B_b}\left[l_{eff} + P_N l_{eff} + \frac{2\beta_{eff}P_N}{B_b}\right]^2 + (1 - P_N)^2\left(B_b^2 \sigma^2_{l_{eff}} + \sigma^2_{\beta_{eff}}\right) \tag{6}$$

$$\sigma^2_{\zeta} = \left[(B_b l_{eff} + \beta_{eff})P_N\right]^2 \left[2^2\left(\frac{\sigma^2_{R_b}}{R_b^2} + \frac{\sigma^2_{R_a}}{R_a^2} + \frac{\sigma^2_{B_a}}{B_a^2}\right) + \frac{\sigma^2_{C_b} + \sigma^2_{\Phi_b}}{(\Phi_b - C_b)^2} + \frac{\sigma^2_{C_a} + \sigma^2_{\Phi_a}}{(\Phi_a - C_a)^2}\right] \\ + \sigma^2_{B_b}\left[P_N l_{eff} + \frac{2\beta_{eff}P_N}{B_b}\right]^2 + P_N^2\left(B_b^2 \sigma^2_{l_{eff}} + \sigma^2_{\beta_{eff}}\right) \tag{7}$$

where the sub-indexes *a* and *b* have the same meaning as before and it was assumed that all the parameters are uncorrelated.

The quantities measured or inferred from the experiments are: *R*, *B*; $\Phi^p$, and *C*. $\beta_{eff}$ and $\Lambda$ were taken from a previous benchmark accepted for publication in the IRPhE project [11] and were assumed independent of the subcriticality level. Thus, through Eq. (3), (4) and (5), the parameters $\zeta$ and $\rho_{gen}$ can be obtained in a purely experimental way. No correction factors of any sort are employed in the measurement procedure.

The same procedure was applied to the CPSD case but in this the parameter C is equal to zero and the countings of the two detectors are now taken into consideration. The relative power in this case is given by:

$$P_N = \frac{R_{1b} R_{2b} \alpha_a^2 (\Phi_a^p)}{R_{1a} R_{2a} \alpha_b^2 (\Phi_b^p)}\ , \tag{8}$$

where $R_{ij}$ is the detector *i* countings in steps *j*, and the other symbols have the same meaning as before.

The Rossi-α case was employed following its standard definition [12] given by:

$$p_{Rossi}\,(\tau) = A + Be^{-\alpha\tau}\ , \tag{9}$$

where

$$A = \epsilon_g \epsilon_c F^2 dt_g dt_c \tag{10}$$

$$B = \frac{\epsilon_g F dt_g \epsilon_c dt_c}{2\alpha\Lambda^2}, \tag{11}$$

where $\epsilon_g$is the detector efficiency: "trigger", $\epsilon_c$ is the detector "counter", $D$ is the Diven factor [13] e $F$ is the average fission rate in the system.

$F$ can be obtained dividing $A$ by $B$ as:

$$F = \frac{AD}{B2\alpha\Lambda^2} \tag{12}$$

and consequently $P_N$ is given by:

$$P_N = \frac{F_b}{F_a} = \frac{A_b B_a \alpha_a}{A_a B_b \alpha_b}\ , \tag{13}$$

where again here the subscript *a* and *b* refer to steps *a* and *b*.

The $P_N$ uncertainty follows the standard error propagation rule as it is given by:

$$\sigma_{P_N} = \sqrt{\left(\frac{\partial P_N}{\partial A_b}\right)^2 . \sigma_{A_b}^2 + \left(\frac{\partial P_N}{\partial B_a}\right)^2 . \sigma_{B_a}^2 + \left(\frac{\partial P_N}{\partial \alpha_a}\right)^2 . \sigma_{\alpha_a}^2 + \left(\frac{\partial P_N}{\partial A_a}\right)^2 . \sigma_{A_a}^2 + \left(\frac{\partial P_N}{\partial B_b}\right)^2 . \sigma_{B_b}^2 + \left(\frac{\partial P_N}{\partial \alpha_b}\right)^2 . \sigma_{\alpha_b}^2} \tag{14}$$

The parameters A, B, and α´s are assumed to be uncorrelated.

## 4. The measurement method and experimental results

A diagram of the electronic equipment and the data acquisition and processing system is illustrated in Figure 2. This figure is the set up for the IPEN/MB-01 correlator.

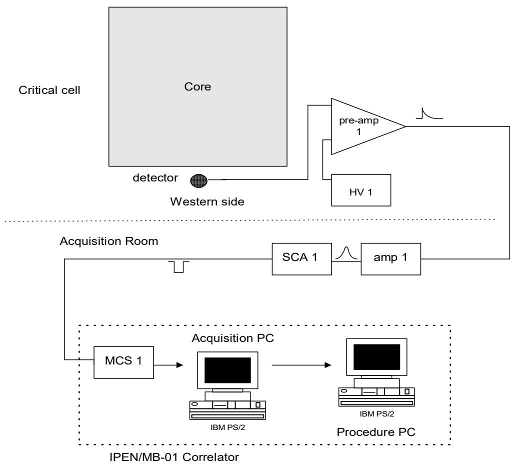


Fig 2. Diagram of electronics and acquisition and data processing system

According to Figure 2, neutron pulses from the detectors are formatted and amplified by preamplifiers and amplifiers and subsequently discriminated from the γ-radiation through the

Lower Level Discriminator of the single channel module (Single-Channel Analyzer - SCA). Negative logical pulses are generated in the output of the single channel (standard NIM fast negative) with 25 ns width and -5 V of amplitude on 50 Ω impedance. A multichannel scaler (MCS) board registers the logical pulses in a number of small time intervals - called dwell time. This procedure is totally analogous to Kitamura's work [14]. The minimum value for the dwell time of the MCS is 100 ns and the number of channels can vary from 4 to 65,536. The dwell time provides the maximum frequency to be analyzed, and the number of channels gives the corresponding frequency resolution. In this work the dwell time was set at $125x10^{-6}$ seconds, which results in a maximum frequency of 4 kHz (single-sided spectrum), and the number of channels, in the time domain, was set to be 65536 (double sided), which results in a resolution of nearly 1 Hz in the frequency domain. Each experimental point of the APSD has an error bar given by $N^{-1/2}$(%), where $N$ is the number of averages. The CPSD shares the same experimental setup of the APSD. For the Rossi-Alpha measurements the dwell time was set to $1x10^{-6}$ so that one pulse could be detected in one channel and a total number of 65536 channels was set.

The detectors employed in the experiments are shown in Table 1.

| Detector ID | Brand | Type | Operating Voltage (kV) | Shaping Time (μs) | Sensitivity (cps/nv) |
|---|---|---|---|---|---|
| 787 | Reuters-Stokes | $BF_3$ | 1.7 | 0.5 | 13 |
| 788 | Reuters-Stokes | $BF_3$ | 1.7 | 0.5 | 13 |
| 8741 | Centronics | $^3He$ | 1.6 | 1.0 | 181 |
| 8742 | Centronics | $^3He$ | 1.6 | 1.0 | 181 |

Tab 1: Detector Type and Specifications

Table 2 shows the case number and its descriptions including measured boron concentrations, the detector types employed in the measurements and their locations. The case "0" is not subcritical; instead, it has a positive reactivity excess of 10 pcm when all control banks are fully withdrawn. The total reactivity was measured relatively to this case. The first subcritical case is case 1.

<table>
<tr><th>Case</th><th>Control Bank Position (% withdrawn)</th><th>Measured Boron Concentration (ppm)</th><th>Detector Type</th><th>Position</th></tr>
<tr><td>0</td><td>100</td><td>0.0</td><td>-</td><td>-</td></tr>
<tr><td rowspan="2">1</td><td rowspan="2">93</td><td rowspan="2">0.0</td><td rowspan="2">$BF_3$</td><td>D1 – 787</td></tr>
<tr><td>D2 - 788</td></tr>
<tr><td rowspan="4">2</td><td rowspan="4">93</td><td rowspan="4">47.9</td><td rowspan="2">$BF_3$</td><td>D1 – 787</td></tr>
<tr><td>D2 - 788</td></tr>
<tr><td rowspan="2">$^3He$</td><td>D1 - 8741</td></tr>
<tr><td>D2 - 8742</td></tr>
<tr><td rowspan="2">3</td><td rowspan="2">93</td><td rowspan="2">88.9</td><td rowspan="2">$^3He$</td><td>D1 - 8741</td></tr>
<tr><td>D2 - 8742</td></tr>
<tr><td rowspan="2">4</td><td rowspan="2">93</td><td rowspan="2">136.5</td><td rowspan="2">$^3He$</td><td>D1 - 8741</td></tr>
<tr><td>D2 - 8742</td></tr>
<tr><td rowspan="2">5</td><td rowspan="2">93</td><td rowspan="2">185.1</td><td rowspan="2">$^3He$</td><td>D1 - 8741</td></tr>
<tr><td>D2 - 8742</td></tr>
<tr><td rowspan="2">6</td><td rowspan="2">93</td><td rowspan="2">245.2</td><td rowspan="2">$^3He$</td><td>D1 - 8741</td></tr>
<tr><td>D2 - 8742</td></tr>
<tr><td rowspan="2">7</td><td rowspan="2">93</td><td rowspan="2">286.8</td><td rowspan="2">$^3He$</td><td>D1 - 8741</td></tr>
<tr><td>D2 - 8742</td></tr>
</table>

Tab 2: Case number and their description

The experiment considered eight cases as shown in Table 2. The starting subcritical case (case 1) has to satisfy the following conditions: a) be a subcritical state, b) be as close as possible to the critical state, and c) be farther away from the critical state so that the experimental detectors do not reach saturation conditions. The 93% control bank withdrawn position was found to be satisfactory to initiate the experiment because it satisfies the initial conditions stated previously. This control bank position remained fixed throughout the experiment. The perturbation was considered between cases.

Figure 3 shows the experiment evolution. The first case refers to the core with the control fully withdrawn. The second one is the beginning of the subcritical experiment. The subsequent cases consider the moderator doped with boric acid ($H_3BO_3$). The subcriticality index ($\zeta$) is always determined at the beginning of each case. The generalized reactivity ($\rho_{gen}$) is determined between consecutive subcritical cases. The reactivity between case 1 and case "0" was taken equal to $-\zeta$ since close to criticality $\rho_{gen}$ and $-\zeta$ are practically equal. The total reactivity is then the sum of all partial reactivities including the 10 pcm of case "0".

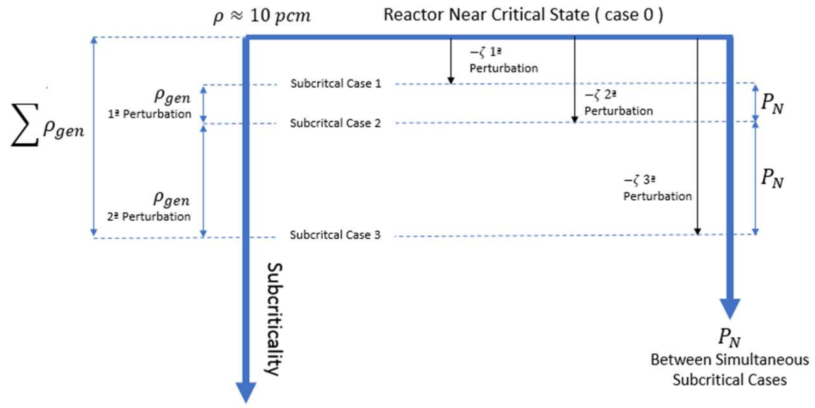


Fig 3. Experiment flowchart

For each case the APSD and CPSD were measured employing the IPEN/MB-01 correlator as shown in Figures 2 and 3. Rossi-α measurements were performed starting in case 3 due to the requirements of keeping dwell time constant for all cases. The counting rates are too high for the first cases and the dwell time for these cases would be significantly different.

Figure 4 shows examples of the APSD measurements for cases 2 and 3 including the results of the least square fit. The results were obtained from the data measured in the detector 8741 (position D1).

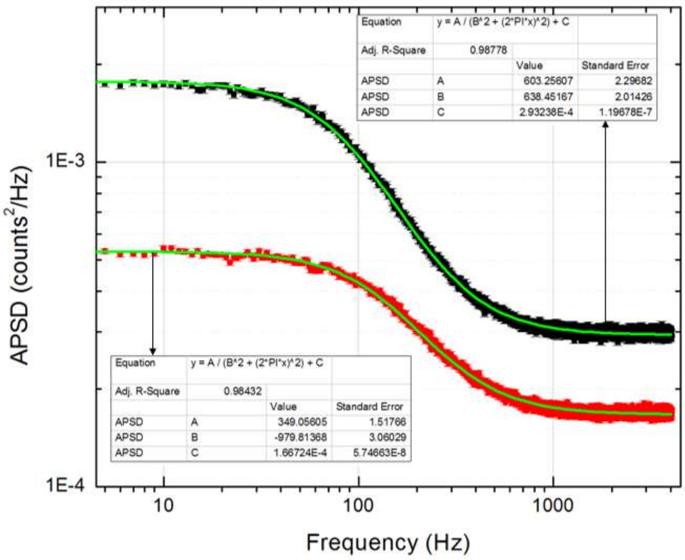


Fig 4. Spectral densities for cases 2 (Black) and 3 (Red)

Tables 3 and 4 show, respectively, the subcriticality index ($\zeta$) and the total generalized reactivity ($\sum \rho_{gen}$) for each case. The total generalized reactivity is relative to case "0" as stated previously. Both the subcriticality index ($\zeta$) and the sum of the generalized reactivity ($\sum \rho_{gen}$) were determined with excellent levels of accuracy.

The subcriticality index ($\zeta$) shows a good agreement among all types of measurements performed in this work. The Rossi-α measurements starts in case 3. The first $\rho_{gen}$ was obtained between cases 3 and 4. In this case it was assumed that $-\zeta$ of case 3 was the total reactivity up to this case. The agreement among the APSD´s and Rossi-α total reactivity measurements were very good and inside of the 1-σ interval of the experimental uncertainty. The same can not be said for the CPSD measurements which diverge from the APSD and Rossi-α measurements. The main reason for that is the relative power ($P_N$) which was strongly dependent on the frequency cutoff. This parameter was very difficult to be determined from the spectral data. The experimental data at high frequency shows very high dispersion with very poor resolution when the subcriticality level gets more and more deep.

There is a fundamental difference between the subcriticality index and the total reactivity. The subcriticality level is proportional to the relative power $P_N$ and the total reactivity is proportional to (1- $P_N$). However, since $P_N$ in general is very close to 1.0, the value of (1- $P_N$) is much more dependent on the quality of $P_N$ determination than the value of $P_N$ itself. That is the main reason for the better agreement of the determination of the subcritical index for the CPSD case than that for the total reactivity.

| Case | Rossi-α | | CPSD | | APSD – (D1) | | APSD – (D2) | |
|---|---|---|---|---|---|---|---|---|
| | $\zeta$ (pcm) | $\sigma_\zeta$ (pcm) | $\zeta$ (pcm) | $\sigma_\zeta$ (pcm) | $\zeta$ (pcm) | $\sigma_\zeta$ (pcm) | $\zeta$ (pcm) | $\sigma_\zeta$ (pcm) |
| 1 | - | - | 133 | 7 | 122 | 4 | 100 | 6 |
| 2 | - | - | 1,287 | 36 | 1,168 | 30 | 1,207 | 32 |
| 3 | 2,335 | 54 | 2,492 | 63 | 2,461 | 62 | 2,198 | 54 |
| 4 | 3,338 | 63 | 3,532 | 88 | 3,483 | 91 | 3,550 | 91 |
| 5 | 4,435 | 75 | 4,447 | 108 | 4,519 | 119 | 4,316 | 115 |
| 6 | 5,546 | 83 | 5,461 | 140 | 5,501 | 154 | 5,509 | 152 |

Tab 3: The subcriticality index ($\zeta$)

| Case | Rossi-α | | CPSD | | APSD – (D1) | | APSD – (D2) | |
|---|---|---|---|---|---|---|---|---|
| | $\sum \rho_{gen}$ (pcm) | $\sigma_{\sum \rho_{gen}}$ (pcm) | $\sum \rho_{gen}$ (pcm) | $\sigma_{\sum \rho_{gen}}$ (pcm) | $\sum \rho_{gen}$ (pcm) | $\sigma_{\sum \rho_{gen}}$ (pcm) | $\sum \rho_{gen}$ (pcm) | $\sigma_{\sum \rho_{gen}}$ (pcm) |
| 1 | - | - | -123 | 6 | -112 | 5 | -108 | 7 |
| 2 | | | -1,299 | 36 | -1,259 | 40 | -1,255 | 40 |
| 3 | -2,335 $(-\zeta)$ | 54 | -2,432 | 48 | -2,474 | 52 | -2,442 | 42 |
| 4 | -3,426 | 60 | -3,208 | 58 | -3,485 | 69 | -3,629 | 64 |
| 5 | -4,625 | 69 | -3,997 | 74 | -4,459 | 98 | -4,622 | 141 |
| 6 | -5,711 | 80 | -4,673 | 93 | -5,456 | 134 | -5,852 | 234 |
| 7 | -6,721 | 93 | -5,304 | 126 | -6,610 | 188 | -6,986 | 383 |

Tab 4: Total generalized reactivity ($\sum \rho_{gen}$)

## 5. Theory/Experiment comparisons

The theory/experiment comparison was performed only for the total generalized perturbation case. Figure 5 shows the theory/experiment comparison. The theoretical part was made by MCNP6.1 [15] employing the ENDF/B-VII.0 library [16]. The agreement among MCNP6.1 calculated values and the APSD´s and Rossi-α measurements were very good and the deviations are inside of the 1-σ interval of the experimental uncertainties.

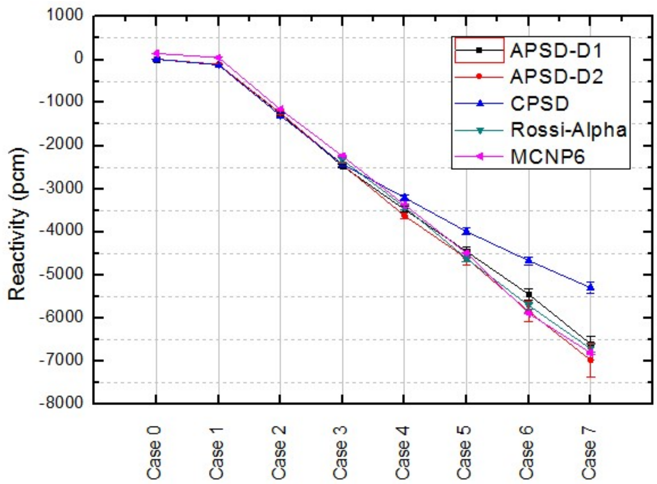


Fig 5. Theory/Experiment comparison

## 6. Conclusions

The boron experiments for the determination of the subcriticality index and the total subcritical reactivity have been successfully performed at the IPEN/MB-01 research reactor facility. The analyses reveal that the experimental results have small uncertainties and they can be considered adequate for a benchmark problem. The measured subcriticality indexes have good agreement among the experimental methods employed in this work. The APSD´s and Rossi-α total reactivity measurements are in a good agreement. The theory/experiment comparison shows very good agreement when the APSD and Rossi-α measurements are considered. The same can not be said for the CPSD total subcritical reactivities. The inference of this parameter from the CPSD measured data shows discrepant results which in some cases are outside of the 1-σ range of the experimental uncertainty of the APSD´s and Rossi-α measured results. The main reason for that is the determination of the relative power ($P_N$) which is very sensitive to the cutoff frequency.

## 7. References


1) Blaise, F. Mellier And P. Fougeras, Application of the Modified Source Multiplication (MSM) Technique to Subcritical Reactivity Worth Measurements in Thermal and Fast Reactor Systems, IEEE Transactions on Nuclear Science, 58(3), 1166-1176, 2011.

2) P. Gajda et. Al. “Correction methods for pulsed neutron source reactivity measurement in accelerator driven systems”, NUKLEONIKA 58(2):287−293, 2013.

3) W. Uyttenhove et. Al. “Detector Positioning for the Initial Subcriticality Level Determination in Accelerator-Driven Systems”, Proceedings of PHYSOR 2012 Advances in Reactor Physics Linking Research, Industry, and Education, Knoxville, Tennessee, USA, April 15-20, 2012, on CD-ROM, American Nuclear Society, LaGrange Park, IL (2012).

4) M. Tsuji, “Subcriticality Measurement by Neutron Source Multiplication Method with a Fundamental Mode Extraction”, Journal of NUCLEAR SCIENCE and TECHNOLOGY, Vol. 40, No. 3, p. 158–169 (March 2003).

5) Sjöstrand, N. G., “Measurement on a subcritical reactor using a pulsed neutron source”, Arkivförfysik, 11, 13 (1956).

6) K. Kumar, “Measurement of sub-critical reactivity in a heavy water reactor by neutron noise methods using a time stamping data acquisition system”, Annals of Nuclear Energy, Volume 87, Part 2, January 2016, Pages 720–727.

7) Gandini, A., “ADS subcriticality evaluation based on the generalized reactivity concept”, Annals of Nuclear Energy. Vol. 31, pp. 813-821, 2004.

8) Dulla, S., et al., “Kinetic Parameters for Source Driven Systems”. PHYSOR-2006. ANS Topical Meeting on Reactor Physics Organized and hosted by the Canadian Nuclear Society. Vancouver, BC, Canada, September, 2006.

9) Gandini, A., 2001. HGPT Based Sensitivity Time-Dependent Method for the Analysis of Subcritical Systems. Annals of Nuclear Energy. Vol. 28, pp. 1193-1217, 2001.

10) A. dos Santos et. al.,” A new experimental approach for subcritical reactivity determination of multiplying systems”, Annals of Nuclear Energy. Vol. 59, pp. 243-254, 2013.

11) Dos SANTOS, A., et. al., IPEN (MB01)-LWR-COEF-KIN-RESR-001: Reactor Physics experiments in the IPEN/MB-01 Research Reactor Facility, in: International Handbook of Evaluated Reactor Physics Benchmark Experiments. Paris: NEA/NSC, pp. 1–142, 2014.

12) R.E. UHRIG, “Random Noise Techniques in Nuclear Reactor Systems, The Ronald Press Company, 1970.

13) Diven, B. C., Martin, H. C., Taschek, R. F., Terrell, J.: Multiplicities of fission neutrons, Phys. Rev., 101, 1012-1015 (1956).

14) Kitamura, Y., Matoba, M., Misawa, T., Unesaki, H., and Shiroya, S., “Reactor Noise Experiments by Using Acquisition System for Time Series Data of Pulse Train,” *J. Nucl. Sci. Technol.*, **36**(8), 653-660 (1999).

15) T. Goorley, et al., "Initial MCNP6 Release Overview", Nuclear Technology, **180**, pp 298-315 (Dec 2012).

16) M.B. Chadwick et al. “ENDF/B-VII.0: Next Generation Evaluated Nuclear Data Library for Nuclear Science and Technology”, Nuclear Data Sheets 107(12):2931-3060, 2006.